Electro-optical and dielectric properties of polymer-stabilized blue phase liquid crystal impregnated with a fluorine-containing compound

Po-Chang Wu [a], Hsin-Li Chen [a], Natalya V. Rudakova [b], Ivan V. Timofeev [c,d], Victor Ya. Zyryanov [c], and Wei Lee [a,*]

[a] *Institute of Imaging and Biomedical Photonics, College of Photonics, National Chiao Tung University, Guiren Dist., Tainan 71150, Taiwan*

[b] *Institute of Engineering Physics and Radio Electronics, Siberian Federal University, Krasnoyarsk 660041, Russia*

[c] *Kirensky Institute of Physics, Siberian Branch of the Russian Academy of Sciences, Krasnoyarsk 660036, Russia*

[d] *Laboratory for Nonlinear Optics and Spectroscopy, Siberian Federal University, Krasnoyarsk 660041, Russia*

(Received

A B S T R A C T

The effects of a fluorine-containing compound (4,4’-difluorobenzophenone; DF) on the electro-optical and dielectric properties of polymer-stabilized blue phase (PSBP) liquid crystals were investigated. When a PSBP cell was driven by an in-plane electric field, the addition of DF up to 2.7 wt% effectively reduced the operation voltage by ~30%. Further inspection by dielectric spectroscopy indicated that the ionic concentration in PSBP decreased with increasing loading of DF. This finding can be ascribed to the adsorption of impurity ions near the ketone group and carbon–fluorine bonds of the DF compound that restrained the ion transport after photopolymerization. As a result, the DF compound can be regarded as a superior ion-suppressor, enabling the reduction in the ionic effect and, in turn, the promotion of the electro-optical response of a PSBP.

Keywords: Polymer-stabilized blue phase, liquid crystal, fluorine-containing compound, operating voltage, ionic effect

---

*wlee@nctu.edu.tw

1. Introduction

Blue phases (BPs) are frustrated liquid crystal (LC) mesophases, existing between the cholesteric and isotropic phases in highly chiral LCs. BPs are composed of double twisted cylinders and disclinations, self-assembling into periodically cubic structures in BPI and BPII or amorphous fog-like framework in BPIII. Because disclinations or defect lines with high free-energy cost are thermodynamically unstable, pristine BP structures can only be preserved within a narrow temperature range, typically 1–5 °C [1, 2]. To date, several approaches, such as forming polymer networks, doping nanoparticles, and using bent-shape LCs, have successively been developed to tackle this inherent problem in BPs. Among them, polymer stabilization of BPs, rendering polymer-stabilized BPs (PSBPs) created by the *in-situ* polymerization of monomers in BPs, has been recognized as an effective way to significantly broaden the temperature range of BPs with excellent durability and reliability [3]. Since Kikuchi *et al.* first demonstrated a PSBP boasting a 60 °C temperature span and a fast electro-optical (EO) response [4], PSBPs have widely been suggested for a variety of technological applications owing to the uniquely structural nature of BPs. For instance, PSBPs, with luring features including stimuli-responsive Bragg reflection-bandgap properties, polarization-insensitive optical isotropy, and fast EO Kerr switching, have extensively been investigated for designing various optoelectronic and tunable photonic devices [5–8]. More attractively, PSBPs offer many advantages in terms of display properties, such as the submillisecond response time, excellent dark state in the field-off state, wide viewing and no need of alignment layer, permitting their emergence as one of promising materials for realizing next-generation displays [9–11]. Unfortunately, implementations of PSBP in the display industry or

general photonics industry are practically impeded by several fatal drawbacks, especially such as the undesired high driving voltage, EO hysteresis, and residual birefringence [12–14].

In view of fabrication processes of conventional PSBP, the combination of a diacrylate monomer (e.g. RM257) with triarylate (e.g. TMPTA) or monoarylate monomer (e.g. EHA or C12A) has largely been adopted as a primary element to construct polymer networks for BP stabilization after the photopolymerization. Typically, increasing the monomer concentration can readily repress the hysteresis and residual birefringence and shorten the response time of a PSBP but the trade-off is the considerable increase in operation voltage [15]. As such, the effects of photopolymerization conditions—in association with the curing temperature [16], the light source [17, 18], the cooling rate [19] and indispensable substances including the LC host and chiral dopant [20], monomer type and concentration [15, 21–23], and photoinitiator [24]—on the display characteristics of PSBPs have been explored and optimal conditions identified. Alternatively, using low molecular-weight [25] or low-surface-tension monomer [26] as one of the components in the prepolymer matrix has also been suggested to reduce the driving voltage as well as the response time through the increase in the Kerr constant or to suppress the hysteresis. Moreover, designing the electrode with unconventional structures (beyond the typically two-dimensional, parallel stripes) for generating strong and deep-penetrating in-plane electric fields [27, 28] and replacing the commonly employed in-plane-switching (IPS) mode by the vertical-field-switching (VFS) mode for supplying uniform longitudinal electric fields [29] have been proposed to significantly lower the operation voltage, suppress the voltage–transmittance hysteresis and shorten the response time.

In this work we focus on the properties of PSBPs and consider the effect of the incorporation of an organic fluorine-containing compound (4,4’-difluorobenzophenone or bis(4-fluorophenyl)methanone; DF) of molecular weight of 218.20 g·mol^{-1} together with two commonly used monomers RM257 and TMPTA into a BP mixture. After performing photopolymerization of the ternary mixture by ultraviolet (UV) light exposure, the effects of DF on the EO and dielectric responses of the PSBP samples were examined. To date, fluorine-containing monomers have been exploited in polymer-dispersed LC systems to improve morphological and EO properties [30–32]. For BPs, only a few studies show an enlarged temperature range of BP by using a host material with lateral fluoro substituents [33] or using a fluorinated chiral dopant in a BP mixture [34]. In the present work, the reduced operation voltage and suppressed ionic effect by addition of DF in PSBPs are, respectively, confirmed in IPS and VFS cells based on the results of the voltage-dependent transmission curves and dielectric spectra.

2. Experimental

The materials used to form a blended PSBP precursor comprise a BPLC mixture, two kinds of photocurable monomers—RM257 (HCCH) and TMPTA (HCCH), a fluorine-containing compound (DF, Alfa Aesar), and the photoinitiator Irgcure 184 (HCCH). Five precursors were prepared for investigations and their detailed compositions are listed in Table 1. Note that “RT” in the sample code RT*x*DF*y* stands for the RM257/TMPTA mixture and the number right behind indicates the concentration of the binary prepolymer in weight per-mille (wt‰). As displayed in Table 1, the total concentration of the three compounds in each PSBP precursor; i.e., $x + y$, is fixed at 9.6

wt%, except for the counterpart RM69DF00. The ratio between the amounts of RM257 and TMPTA was set to 1:1. In other words, when the concentrations of DF are 0, 0.70, 1.70, and 2.70 wt%, the concentrations of RM257 and TMPTA are identically 4.80, 4.45, 3.95, and 3.45 wt%, respectively. The BPLC is composed of a nematic host (HDE, HCCH) and a right-handed chiral additive (R5011, HCCH) in a weight ratio of 96.8:3.2. The nematic host exhibits a clearing point T_c = 97 °C, birefringence Δn = 0.204 (at the wavelength λ = 589 nm and temperature T = 20 °C), and dielectric anisotropy $\Delta\varepsilon$ = 60.64 (at the frequency of 1 kHz and T = 25 °C) [35].

Fig. 1 illustrates the chemical structures of the two monomers and the dopant DF used. RM257 is a diacrylate reactive mesogen showing a core chain and two alkene groups (namely, the carbon–carbon double bonds) in the molecular structure and it is often employed as a cross-linker to form three-dimensional polymer networks [36]. TMPTA is a low-viscosity, low-volatility liquid monomer with three acrylate groups as the reactive sites; it has been proven responsible of providing rigidity and high crosslinking density of the resulting network [37]. In this study, RM257 and TMPTA are the primary components for constructing the main polymer skeletons in PSBP samples. In contrast, DF is a class of difluoro compound, consisting of eight hydrogen atoms, 13 carbon atoms, one oxygen atom, and two fluorine atoms. It is generally used as a precursor for synthesis of poly(etheretherketone) (PEEK) [38].

The PSBP precursors were heated to their isotropic phase and stirred for 2 h to ensure complete liquefaction and uniformity. They were then injected into empty cells by capillary action in the isotropic phase. Here, the cells used are of two types, differing in the electrode design. The IPS cells were made for the EO study whereas the VFS cells forming parallel-plate capacitors for the dielectric investigation. An IPS cell was

assembled with two glass substrates, one of which coated with interdigital indium–tin-oxide (ITO) electrodes (width/spacing = 5 μm/5 μm) while a VFS cell was made of two identical ITO-coated substrates with an effective electrode area of 1 cm^2. The cell gaps of the IPS and the VFS cells were 5.8 μm and 4.5 μm, respectively. Note that no aligning agent was used in this study. Phase sequences of the PSBP precursors were preliminarily inspected by polarizing optical microscopy to identify the temperature ranges of BPs, as given in Table 1. For the fabrication of PSBP samples from their precursors, each cell was heated to the isotropic state and consecutively cooled to the BP with a cooling rate of 0.1 °C/min using a precise temperature controller (Linkam, T95-PE). When obtaining the BP at a designated temperature near the BP-to-cholesteric transition point, each cell was exposed to UV light at λ = 365 nm and intensity of 85 $mW \cdot cm^{-2}$ for 10 min to accomplish the photopolymerization process and thus a PSBP resulted.

EO features of PSBPs were determined by the voltage-dependent transmission (*V*–*T*%) curves of IPS cells. In the EO measurement, an IPS cell was placed between crossed polarizers and the long stripes of interdigital electrodes were set at 45° from the transmission axis of either polarizer. A He–Ne laser beam with emission wavelength at 632.8 nm normally impinged onto the substrate plane of the cell. The intensity of the monochromatic light after passing through the cell was monitored by a photodetector. To prevent the light loss from the diffraction, a convex lens was situated in front of the photodetector to effectively collect diffracted light of distinct orders [39]. On the other hand, ionic properties of PSBPs were investigated in terms of their complex dielectric spectra ($\varepsilon^*(f)$) of VFS cells in the frequency regime between 1 Hz and 10 kHz using a LCR meter (HIOKI 522-50 LCR HiTESTER). Here, $\varepsilon^*(f)$ is defined as $\varepsilon^*(f) = \varepsilon'(f) - i\varepsilon''(f)$, where ε' is the real-part and ε'' the imaginary-part dielectric permittivity. The probe

voltage was as small as 0.3 V_{rms} in the sinusoidal waveform to avoid the contribution of field-induced molecular reorientation to the complex dielectric data.

3. Results and discussion

The stabilization of BP in our PSBP samples was checked with a polarizing optical microscope (Olympus BX51). Fig. 2 displays optical textures of three such samples (with different monomer compositions) before and after photopolymerization. The six micrographs clearly reveal that the BPs appearing at specific temperatures higher than the room temperature prior to polymerization (top row) can successfully be preserved in a widened temperature range covering 25 °C after photopolymerization. Noticeably, the platelet sizes in RT69DF00 are comparable to those in RT69DF27. This implies that the fluorine-containing compound DF does not affect the BP formation, which is totally different from those materials used in Ref. 26. To investigate the effect of DF on the EO properties of PSBPs, IPS samples were driven by square-wave voltages at 1 kHz using an arbitrary function generator (Tektronix AFG-3022B) in conjunction with an amplifier (TREK Model 603).

Fig. 3 depicts the *V*–*T*% curves of five samples at ambient temperature. For samples without DF, the voltage (V_{max}) corresponding to maximum transmittance and the light leakage at V = 0 V_{rms} of the sample RT96DF00 are, respectively, higher than and lower than those of RT69DF00. Such a result is in good agreement with previous studies. It has been suggested that the higher monomer concentration furnishes a stiffer polymer system, thereby yielding a more optically isotropic BP structure at null voltage and causing a higher operating voltage to induce lattice distortion [11, 15]. With fixed overall

prepolymer/DF concentration at 9.6 wt%, partial replacement of RT and TMPTA by DF leads to the reduction in operation voltage of the PSBP. It can be determined from Fig. 3 that the values of V_{max} of samples RT89DF07 (V_{max} = 42 V_{rms}), RT79DF17 (V_{max} = 37 V_{rms}), and RT69DF27 (V_{max} = 32 V_{rms}) are 8.7 %, 19.6 %, and 30.4 % lower than that of sample RT96DF00 (V_{max} = 46 V_{rms}). When comparing samples with identical RT concentration, V_{max} of sample RT69DF27 is lower than that of sample RT69DF00 (V_{max} = 40 V_{rms}) whereas light leakages in the two samples are comparable. This indicates that using DF to minify the operation voltage is actually accompanied by increased light leakage. Such a drawback can be compensated by utilizing a circular polarizer instead of linear polarizer to increase the contrast ratio in that PSBP possesses slight optical rotatory power of double twist cylinders [40]. It can be concluded from the above discussion that the reduction in operation voltage for driving a PSBP can be effectively realized by adding DF into the initial monomer mixture.

Furthermore, Fig. 4 shows the *V*–*T*% curves of three selective samples for comparisons of EO hysteresis and residual birefringence. The RT96DF00 cell is nearly hysteresis-free and exhibits virtually zero residual birefringence. The reduction in RT concentration to 6.9 wt% results in apparent hysteresis and residual birefringence in the voltage regime between 0 V_{rms} and 20 V_{rms}, presumably due to the weakened stability of the polymer network. With the combination of 2.7-wt% DF and 6.9-wt% RT for polymerization, both the hysteresis and residual birefringence are notably suppressed in sample RT69DF27. This means that DF filled together with RT in disclination defects could also play a role in promoting the stiffness of polymer chains but it is not as good as RT.

Previously, the reduced operation voltage of a PSBP by optimizing the monomer

type has been explained by the modified anchoring energy between the LC molecules and polymers. In our case, it might also be attributable to the suppressed ionic behaviors in view of the material characteristics of DF. Generally, ions are unavoidable impurities in a LC cell because they primarily originate from the LC substance used. It is well known that the served ionic effect in a LC cell can establish a significant internal field by the buildup of electrical double layer to counteract the external one, giving rise to the increase in driving voltage. Fig. 5 demonstrates the complex dielectric spectra of three VFS samples (RT69DF00, RT96DF00 and RT69DF27) to allow preliminary examinations of the influence of DF on the ionic behaviors. In the frequency range where the ion transport in the LC bulk can respond to the alternate inversion of electrical polarity of the probe voltage, both $\varepsilon'(f)$ and $\varepsilon''(f)$ dominated by the space-charge polarization vary with $f^{-3/2}$ and f^{-1}, respectively [41], where f is a linear frequency. Consequently, in contrast to the results of those samples without DF, the shift of the $\varepsilon'(f)$ (Fig. 5(a)) and $\varepsilon''(f)$ (Fig. 5(b)) curves to lower frequencies of the RT69DF27 sample briefly suggests the curbed ion transport and, hence, the restrained ionic effect. To quantitatively determine the ionic behavior as a function of the DF concentration, we follow a theoretical model established by Barbero *et al.* [42] to deduce the ion density n and diffusivity D in the cell by fitting the experimental data of $\varepsilon'(f)$ and $\varepsilon''(f)$ into the following equations [43]:

$$\varepsilon' = \frac{nq^2 D^{3/2}}{\pi^{3/2}\varepsilon_0 d k_B T} f^{-3/2} + \varepsilon'_b \tag{1}$$

and

$$\varepsilon' = \frac{nq^2 D}{\pi\varepsilon_0 k_B T} f^{-1}, \qquad \varepsilon'' = \frac{nq^2 D}{\pi\varepsilon_0 k_B T} f^{-1} \tag{2}$$

where q is the electric charge, d is the cell gap, ε_0 is the permittivity in free space, k_B is

the Boltzmann constant, T is the absolute temperature, and $\varepsilon_{\perp}'$ is the intrinsic dielectric constant of the LC bulk. According to the experimental results of the VHS-PSBP samples with identical total RM257/TMPTA/DF concentrations of 9.6 wt% listed in Table 2, D remains nearly constant (varying between 1.98×10^{-6} $cm^2 \cdot s^{-1}$ and 2.26×10^{-6} $cm^2 \cdot s^{-1}$) but n decreases from 39.6 $\mu C \cdot cm^{-3}$ to 20.0 $\mu C \cdot cm^{-3}$, revealing a ~50 % reduction in n, as the content of DF increases from 0 to 2.7 wt%. By calculating distributed partial charges in the DF molecule using Chem3D (CambridgeSoft®), the oxygen and fluorine atoms with negative partial charges are labeled in Fig. 6. In the polymerization process, the C=O bond of DF will not cleave and should not react with RM257 and TMPTA as the reactivity of the ketone group is low. For polymerization of DF to occur, other reactants should be added, such as in the preparation of PEEK [38]. (The fluoride group of DF may be reactive in substitution reactions, but the alkene groups (C=C) in RM257 and TMPTA are not suitable for such reaction.) The oxygen and fluorine atoms in the carbon–oxygen and carbon–fluorine bonds of dispersed DF molecules with negative partial charges could thus be accountable to the adsorption of impurity ions to restrain the ion transport. Although DF is confirmed to reduce the ionic effect and lower the operation voltage, replacing all the contents of RM257 and TMPTA by DF is not suggested because this compound alone can hardly stabilize the BP state at room temperature.

4. Conclusions

In conclusion, PSBP cells with wide BP temperature ranges covering the room temperature were fabricated by adopting distinct amounts of a third compound (DF) together with two monomers (RM257 and TMPTA) into the BP mixture, followed by

photopolymerization. A series of experiments were then conducted to study the effects of DF concentration on the EO and dielectric properties of PSBP cells. By fixing the overall concentration of the three compounds (RM257/TMPTA/DF) at 9.6 wt%, the experimentally obtained *V*–*T*% curves indicate that the operation voltage of IPS-PSBP cells decreases with increasing DF concentration from 0 wt% to 2.7 wt%. Our data also suggest that DF dispersed in the precursor could be also responsible for the enhancement of the stiffness of the resulting polymer networks in that the EO hysteresis and residual birefringence of RT69DF00 is suppressed due to the incorporation of 2.7 wt% DF. Furthermore, the mechanism of improved EO performance of PSBPs by adding DF can be explained in terms of the modification in ionic behavior. By means of dielectric spectroscopy, it is found that the ionic effect in PSBP samples is weakened with increasing DF concentration. Quantitatively speaking, increasing the DF concentration from 0 to 2.7 wt% results in the ion density to fall from 39.6 μC·cm^{-3} to 20.0 μC·cm^{-3}. By confirming the presence of partial charges on the ketone and fluoride groups, such a result could be explained by the adsorption of impurity ions near the carbon–oxygen and carbon–fluorine bonds of DF. Consequently, with the aim towards the promotion of PSBP for practical uses, this study provides a new pathway from the point of view of material optimization for improved EO responses of a PSBP.

Acknowledgments

This work was financially supported by the Ministry of Science and Technology, Taiwan, through Grant Nos. 104-2112-M-009-008-MY3 and 106-2923-M-009-002-MY3, and by the Russian Foundation for Basic Research, Government of Krasnoyarsk Territory,

Krasnoyarsk Region Science and Technology Support Fund to the research projects 16-42-240704 and 17-42-240464.

References

[1] S. Meiboom, J.P. Sethna, P.W. Anderson, W.F. Brinkman, Theory of the blue phase of cholesteric liquid crystals, Phys. Rev. Lett. **46** (1981) 1216–1219.

[2] S. Meiboom, M. Sammon, W.F. Brinkman, Lattice of disclinations: The structure of the blue phases of cholesteric liquid crystals, Phys. Rev. A **27** (1983) 438–454.

[3] G. Nordendorf, A. Hoischen, J. Schmidtke, D. Wilkes, H.-S. Kitzerow, Polymer-stabilized blue phases: promising mesophases for a new generation of liquid crystal displays, Polym. Adv. Technol. **25** (2014) 1195–1207.

[4] H. Kikuchi, M. Yokota, Y. Hisakado, H. Yang, T. Kajiyama, Polymer-stabilized liquid crystal blue phases, Nat. Mater. **1** (2002) 64–68.

[5] Y. Li, S. Huang, P. Zhou, S. Liu, J. Lu, X. Li, Y. Su, Polymer-stabilized blue phase liquid crystals for photonic applications, Adv. Mater. Technol. **1** (2016) 1600102.

[6] T.-H. Lin, Y. Li, C.-T. Wang, H.-C. Jau, C.-W. Chen, C.-C. Li H. K. Bisoyi, T. J. Bunning, Q. Li, Red, green and blue reflections enabled in an optically tunable self-organized 3D cubic nanostructured thin film, Adv. Mater. **25** (2013) 5050–5054.

[7] S.-Y. Jo, S.-W. Jeon, B.-C. Kim, J.-H. Bae, F. Araoka, S.-W. Choi, Polymer stabilization of liquid-crystal blue phase II toward photonic crystals, ACS Appl. Mater. Interfaces **9** (2017) 8941−8947.

[8] Y.-H. Lin, H.-S. Chen, T.-H. Chiang, H.-K. Hsu, A reflective polarizer-free electro-optical switch using dye-doped polymer-stabilized blue phase liquid crystals, Opt. Express **19** (2011) 2556–2561.

[9] Z. Ge, S. Gauza, M. Jiao, H. Xianyu, S.-T. Wu, Electro-optics of polymer-stabilized blue phase liquid crystal displays, Appl. Phys. Lett. **94** (2009) 101104.

[10] Y. Chen, J. Yan, J. Sun, S.-T. Wu, X. Liang, S.-H. Liu, P.-J. Hsieh, K.-L. Cheng, J.-W. Shiu, A microsecond-response polymer-stabilized blue phase liquid crystal, Appl. Phys. Lett. **99** (2011) 201105.

[11] J. Yan, L. Rao, M. Jiao, Y. Li , H.-C. Cheng, S.-T. Wu, Polymer-stabilized optically isotropic liquid crystals for next-generation display and photonics applications, J. Mater. Chem. **21** (2011) 7870–7877

[12] Y. Chen, D. Xu, S.-T. Wu, S. Yamamoto, Y. Haseba, A low voltage and submillisecond-response polymer-stabilized blue phase liquid crystal, Appl. Phys. Lett. **102** (2013) 141116.

[13] K. M. Chen, S. Gauza, H. Xianyu, S.-T. Wu, Hysteresis effects in blue-phase liquid crystals, J. Disp. Technol. **6** (2010) 318–322.

[14] Y.-F. Lan, C.-Y.Tsai, J.-K. Lu, N. Sugiura, Mechanism of hysteresis in polymer-network stabilized blue phase liquid crystal, Polymer **54** (2013) 1876–1879.

[15] T.N. Oo, T. Mizunuma, Y. Nagano, H. Ma, Y. Ogawa, Y. Haseba, H. Higuchi, Y. Okumura, H. Kikuchi, Effects of monomer/liquid crystal compositions on electro-optical properties of polymer stabilized blue phase liquid crystal, Opt. Mater. Express **1** (2011) 1502−1510.

[16] C.-Y. Fan, H.-C. Jau, T.-H. Lin, F. C. Yu, T.-H. Huang, C. Liu, N. Sugiura, Influence of polymerization temperature on hysteresis and residual birefringence of polymer stabilized blue phase LCs, J. Disp. Technol. **7** (2011) 615–618.

[17] Y. Liu, S. Xu, D. Xu, J. Yan, Y. Gao, S.-T. Wu, A hysteresis-free polymer-stabilised blue-phase liquid crystal, Liq. Cry. **41** (2014) 1339–1344.

[18] D. Xu, J. Yuan, M. Schadt, S.-T. Wu, Blue phase liquid crystals stabilized by linear photo-polymerization, Appl. Phys. Lett. **105** (2014) 081114.

[19] H.-S. Chen, Y.-H. Lin, C.-H. Wu, M. Chen, H.-K. Hsu, Hysteresis-free polymer-stabilized blue phase liquid crystals using thermal recycles, Opt. Mater. Express **2** (2012) 1149–1155.

[20] L. Rao, J. Yan, S.-T. Wu, S. Yamamoto, Y. Haseba, A large Kerr constant polymer-stabilized blue phase liquid crystal, Appl. Phys. Lett. **98** (2011) 081109.

[21] J. Yan, S.-T. Wu, Effect of polymer concentration and composition on blue phase liquid crystals, J. Disp. Technol. **7** (2011) 490–493.

[22] J.-L. Zhu, S.-B. Ni, C. P. Chen, X.-L. Song, C.-Y. Chen, J.-G. Lu, Y. Su, The Influence of polymer system on polymerstabilised blue phase liquid crystals, Liq. Cry. **41** (2014) 891–896.

[23] T. Mizunuma, T.N. Oo, Y. Nagano, H. Ma, Y. Haseba, H. Higuchi, Y. Okumura, H. Kikuchi, Electro-optical properties of polymer-stabilized blue phase with different monomer combination and concentration, Opt. Mater. Express **1** (2011) 1561–1568.

[24] E. Kemiklioglu, L.-C. Chien, Effects of photoinitiator on electro-optical properties of polymerization-induced phase separation blue-phase liquid crystals, Eur. Phys. J. E **40** (2017) 11524.

[25] J.-L. Zhu, S.-B. Ni, Y. Song, E.-W. Zhong, Y.-J. Wang, C.P. Chen, Z. Ye, G. He, D.-Q. Wu, X.-L. Song, J.-G. Lu, Y. Su, Improved Kerr constant and response time of polymer-stabilized blue phase liquid crystal with a reactive diluent, Appl. Phys. Lett. **102** (2013) 071104.

[26] P.-J. Hsieh, H.-M. Philip Chen, Hysteresis-free polymer-stabilised blue phase liquid crystals comprising low surface tension monomers, Liq. Cry. **42** (2015) 216–221.

[27] M. Kim. M.S. Kim, B.G. Kang, M.K. Kim, S. Yoon, S.H. Lee, Z. Ge, L. Rao, S. Gauza, S.-T. Wu, Wall-shaped electrodes for reducing the operation voltage of

polymer-stabilized blue phase liquid crystal displays, J. Phys. D: Appl. Phys. **42** (2009) 235502.

[28] L. Rao, Z. Ge, S.-T. Wu, S.H. Lee, Low voltage blue-phase liquid crystal displays Appl. Phys. Lett. **95** (2009) 231101.

[29] H.-C. Cheng, J. Yan, T. Ishinabe, S.-T. Wu, Vertical field switching for blue-phase liquid crystal devices, Appl. Phys. Lett. **98** (2011) 261102.

[30] M. D. Schulte, S. J. Clarson, L. V. Natarajan, D. W. Tomlin, T. J. Bunning, The effect of fluorine-substituted acrylate monomers on the electro-optical and morphological properties of polymer dispersed liquid crystals, Liq. Cry. **27** (2000) 467–475.

[31] Z. Zheng, J. Ma, W. Lia, J. Song, Y. Liu, L. Xuan, Improvements in morphological and electro-optical properties of polymer-dispersed liquid crystal grating using a highly fluorine-substituted acrylate monomer, Liq. Cry. **35** (2008) 885–893.

[32] J. Y. Woo, B. K. Kim, Transmission holographic polymer-dispersed liquid crystal based on fluorinated polymer matrices, Liq. Cry. **35** (2008) 987–994.

[33] K. Kakisaka, H. Higuchi, Y. Okumura, H. Kikuchi, A fluorinated binaphthyl chiral dopant for fluorinated liquid crystal blue phases, J. Mater. Chem. **2** (2014) 6467–6470.

[34] B. Li, Wanli He, L. Wang, X. Xiao, H. Yang, Effect of lateral fluoro substituents of rodlike tolane cyano mesogens on blue phase temperature ranges, Soft Matter **9** (2013) 1172–1177

[35] P.-C. Wu, H.-T. Hsu, H.-L. Chen, W. Lee, Dielectric characterization and voltage holding ratio of blue-phase cells, Displays **44** (2016) 66–72

[36] V. Stroganov, A. Ryabchun, A. Bobrovsky, V. Shibaev, novel type of crown ether-containing metal ions optical sensors based on polymer-stabilized cholesteric liquid crystalline films. Macromol. Rapid Commun. **33** (2012) 1875−1881.

[37] H. Hou, Y. Gan, J. Yin, X. Jiang, Polymerization-induced growth of microprotuberance on the photocuring coating, Langmuir, **33** (2017) 2027–2032.

[38] D.J. Adams, J.H. Clark, H. McFarland, The formation of 4,4'-difluorobenzophenone from 4,4'–dinitrodiphenylmethane, J. Fluorine Chem. **92** (1998) 127–129

[39] J. Yan, Y. Li, S.-T. Wu, High-efficiency and fast-response tunable phase grating using a blue phase liquid crystal, Opt. Lett. **36** (2011) 1404–1406.

[40] J. Yan, Z. Luo, S.-T. Wu, J.-W. Shiu, Y.-C. Lai, K.-L. Cheng, S.-H. Liu, P.-J. Hsieh, Y.-C. Tsai, Low voltage and high contrast blue phase liquid crystal with red-shifted Bragg reflection, Appl. Phys. Lett. **102** (2013) 011113.

[41] H.-H. Liu, W. Lee, Time-varying ionic properties of a liquid-crystal cell, Appl. Phys. Lett. **97** (2010) 023510.

[42] G. Barbero, A.L. Alexe-Ionescu, Role of the diffuse layer of the ionic charge on the impedance spectroscopy of a cell of liquid, Liq. Cryst. **32** (2005) 943–949.

[43] F.-C. Lin, P.-C. Wu, B.-R. Jian, W. Lee, Dopant effect and cell-configuration-dependent dielectric properties of nematic liquid crystals, Adv. Cond. Mat. Phys. **271574** (2013) 1–5.

Table 1

Compositions of various BP precursors and their isotropic-to-BP and BP-to-CLC phase transition temperatures.

Sample	BPLC (wt%)	RM257 (wt%)	TMPTA (wt%)	DF (wt%)	lIRG184 (wt%)	$T_{\text{Iso-to-BP}}/T_{\text{BP-CLC}}$ °C/°C
RT69DF00	92.7	3.45	3.45	0	0.40	76.5/68.0
RT96DF00	90.0	4.80	4.80	0	0.40	73.8/63.2
RT89DF07	90.0	4.45	4.45	0.70	0.40	69.7/60.6
RT79DF17	90.0	3.95	3.95	1.70	0.40	68.4/60.2
RT69DF27	90.0	3.45	3.45	2.70	0.40	68.0/59.4

Table 2

Summary of the ion density n and diffusivity D of various PSBP samples at T = 25 °C. Values are obtained by fitting the dielectric data with Eqs. (1) and (2).

Sample	n (10^4 nC·cm^{-3})	D (10^{-6} cm^2·s^{-1})
RT69DF00	3.00	2.89
RT96DF00	3.96	1.98
RT89DF07	3.66	2.20
RT79DF17	2.87	2.26
RT69DF27	2.00	2.06

Figure Captions

Fig. 1. Chemical structures of three mixed compounds: (a) RM257, (b) TMPTA, and (c) 4,4’-difluorobenzophenone (DF), an organic compound with the formula of $(FC_6H_4)_2CO$.

Fig. 2. BP textures of three primary samples (RT69DF00, RT96DF00, and RT69DF27) before polymer stabilization at designated temperatures (top row) and after polymer stabilization at 25 °C (bottom row). The brightness of the photos is increased by 40% to facilitate comparisons.

Fig. 3. Normalized voltage-dependent transmission curves of five IPS-PSBP cells driven by square wave voltages at frequency of 1 kHz. λ = 632.8 nm.

Fig. 4. Normalized *V*–*T*% curves showing hysteresis and residual birefringence of three IPS samples: RT96DF00, RT69DF00, and RT69DF27. λ = 632.8 nm.

Fig. 5. (a) Real- and (b) imaginary-part dielectric spectra of VFS-PSBP samples RT69DF00, RT96DF00, and RT69DF27 at 25 °C.

Fig. 6. Partial-charge distribution in the fluro compound 4,4’-difluorobenzophenone (DF).

Fig. 1

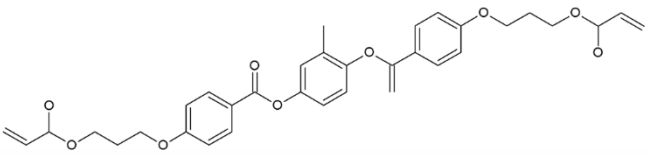

(a) RM257

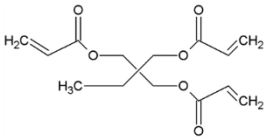

(b) TMPTA

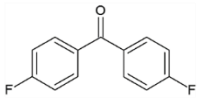

(c) 4,4’-Difluorobenzophenone

Fig. 2

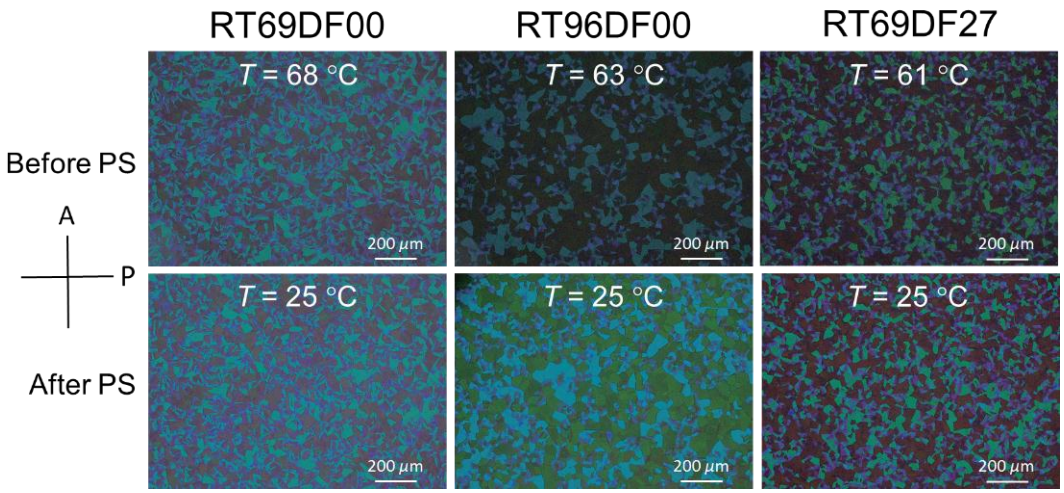
RT69DF00
RT96DF00
RT69DF27
Before PS
A
P
After PS
T = 68 °C
T = 63 °C
T = 61 °C
T = 25 °C
T = 25 °C
T = 25 °C
200 μm
200 μm
200 μm
200 μm
200 μm
200 μm

Fig. 3

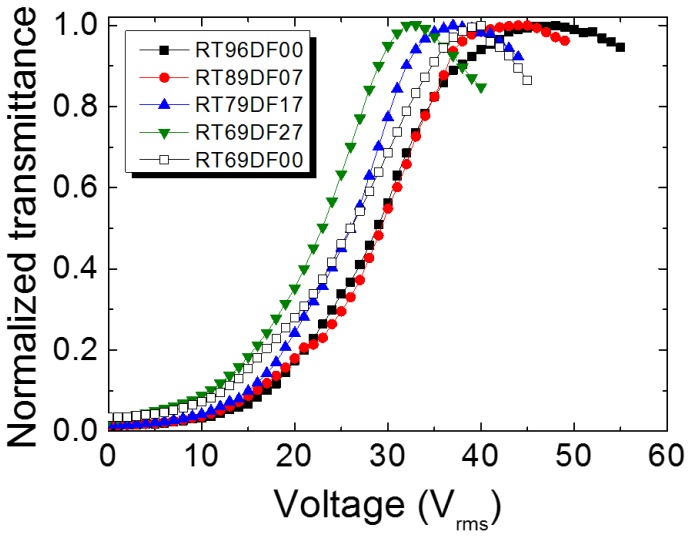
Normalized transmittance
1.0
0.8
0.6
0.4
0.2
0.0
0
10
20
30
40
50
60
Voltage (V rms)
RT96DF00
RT89DF07
RT79DF17
RT69DF27
RT69DF00

Fig. 4

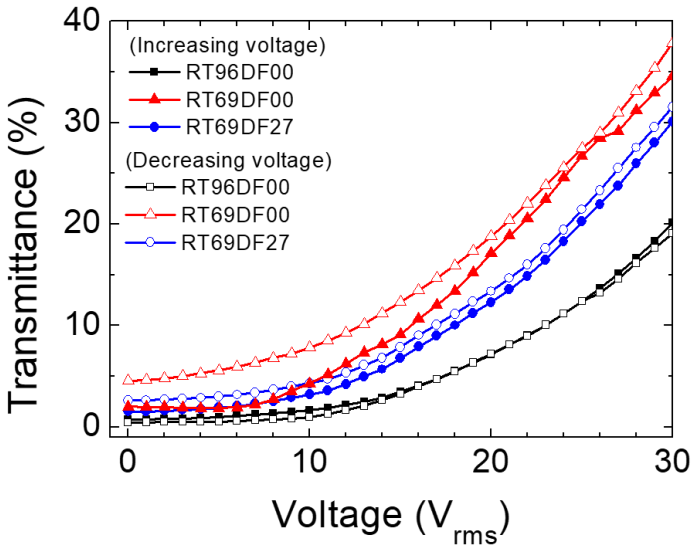
(Increasing voltage)
RT96DF00
RT69DF00
RT69DF27
(Decreasing voltage)
RT96DF00
RT69DF00
RT69DF27
Transmittance (%)
Voltage (V rms)
0
10
20
30
40

Fig. 5

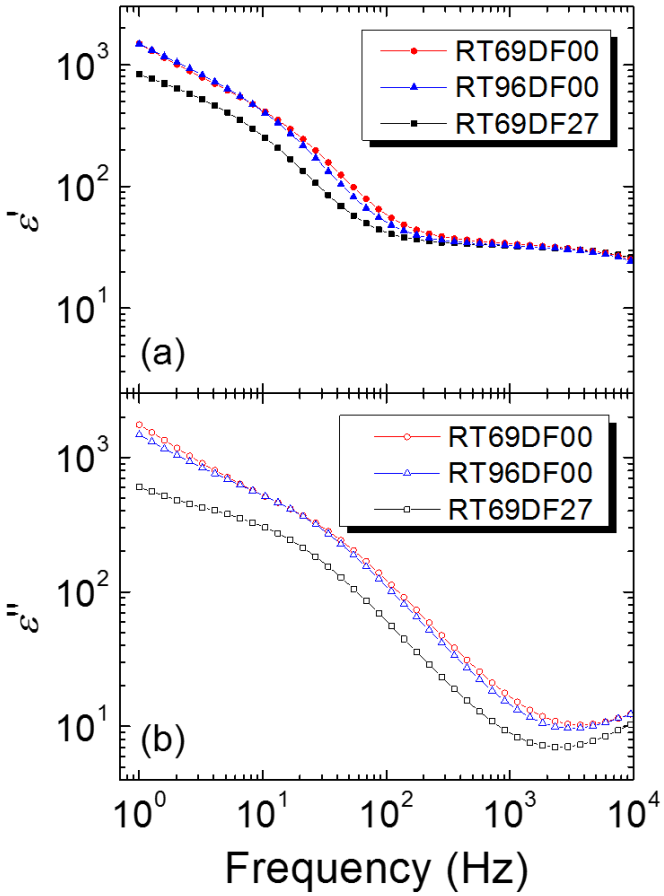

Fig. 6